

## Nonambipolarity of Fluctuation-Driven Fluxes and Its Effect on the Radial Electric Field

W.M. Solomon\* and M.G. Shats

*Plasma Research Laboratory, Australian National University, Canberra ACT 0200 Australia*

(Received 18 June 2001; published 22 October 2001)

The nonambipolarity of the fluctuation-driven particle transport is demonstrated experimentally. Convective radial transport of electrons by fluctuations is found to be significantly stronger than that of ions, leading to a mean fluctuation-driven radial current balanced in steady state by other bipolar particle losses. Fluctuation suppression leads to a sudden disappearance of this current and results in significant modification to the radial electric field. The observed change in the electric field is in good agreement with the measured fluctuation-driven flux.

DOI: 10.1103/PhysRevLett.87.195003

PACS numbers: 52.55.Hc, 52.25.Fi, 52.25.Gj

A complex interplay between turbulent fluctuations and plasma flows has become a focus in fusion plasma research in the context of particle and energy transport and confinement improvement (for reviews, see, for example, [1,2]). This interest is driven mostly by prospects of reducing the turbulent transport and improving the plasma confinement. The effect of the electric field and its radial gradient (shear) on the turbulence-induced transport has been extensively studied both theoretically and experimentally [1,3].  $E \times B$  shear flows seem to be responsible for reduction in the turbulent transport, and thus it is very important to understand the physics of the shear flow formation. Among other mechanisms, turbulence itself can generate plasma flows, for example, through the Reynolds stress mechanism [4] or due to the finite-Larmor-radius (FLR) effect [5,6]. In any case such flow generation would be manifested as the fluctuation-driven radial current  $J_r = e(\langle \tilde{n}_i \tilde{V}_{ri} \rangle - \langle \tilde{n}_e \tilde{V}_{re} \rangle)$ , where  $\tilde{n}_s$  and  $\tilde{V}_{rs}$  are fluctuations of density and radial velocity for electrons ( $s = e$ ) and ions ( $s = i$ ), which can change the radial electric field.

In this Letter we report the first measurements of the nonambipolar fluctuation-driven particle flux and demonstrate its effect on the radial electric field and the particle confinement. The results suggest that fluctuations can dramatically affect the structure of the radial electric field.

Poisson's equation relates the time rate of change of the radial electric field  $E_r$  with all the flux processes that might generate a radial current [2]:

$$\frac{\varepsilon_0 \varepsilon_{\perp}}{e} \frac{\partial}{\partial t} E_r = \sum_{s=i,e} \sum_k \Gamma_s^k, \quad (1)$$

where  $\varepsilon_{\perp}$  represents the perpendicular dielectric constant and the summation over  $k$  is to represent all transport processes in the plasma. These may include neoclassical diffusion, ion orbit loss (substantial in the reported experiments), and fluctuation-driven transport, among others.

The condition of quasineutrality for a plasma requires that the total particle flux is ambipolar. A particular process  $k$  can be said to be ambipolar if  $\Gamma_e^k = \Gamma_i^k$ . However, the quasineutrality of the plasma does not require that

each particular process be ambipolar: a bipolar contribution from one process can be balanced by one (or more) bipolar components from another process.

To test the ambipolarity of the fluctuation-driven fluxes, we propose a technique to independently estimate the two fluxes for the ions and electrons. We perform the experiments on the H-1 heliac [7]. H-1 is a three-field period toroidal heliac with major radius  $R_0 = 1.0$  m and mean minor radius  $a \approx 0.2$  m. Plasma is produced in argon at low magnetic fields ( $< 0.2$  T) using less than 100 kW of rf power. Typical plasma parameters are  $n_e \sim 1 \times 10^{18} \text{ m}^{-3}$ ,  $T_e \sim 10$  eV,  $T_i \sim 40$  eV, and ion gyro radius  $\rho_i \geq 0.2a$  [8].

Mach (or paddle) probes are often used to provide information about plasma flow velocities [9,10]. In the case where the characteristic probe dimension  $r_p$  is less than  $\rho_i$ , the Mach probe is referred to as "unmagnetized." This is the situation for the following experiments on H-1, where  $\rho_i \sim 6$  cm and  $r_p < 0.5$  cm. A theory suitable for unmagnetized Mach probes has been described [11]; however, it is applicable only for  $T_i < T_e$ . This condition is in general not satisfied in H-1; however, the theory is readily extended to cover this. An expression relating the ratio of the upstream ( $I_s^+$ ) and downstream ( $I_s^-$ ) ion saturation currents  $R = I_s^+ / I_s^-$  to the ion drift velocity is given by [12]

$$V_{di} = \bar{V}_{di} + \tilde{V}_{di} = \frac{\pi q (\bar{T}_e + \tilde{T}_e) \ln(\bar{R} + \tilde{R})}{4m(\bar{V}_{ti} + \tilde{V}_{ti})}, \quad (2)$$

where  $q$  is the ion charge,  $m$  is the ion mass,  $V_{ti}$  is the ion thermal velocity, the bar represents time-averaged quantities, and the tilde represents fluctuating quantities.

Since the Mach probe is unmagnetized, it may be oriented to be sensitive to the ion radial velocity  $V_{ri}$  and its fluctuations  $\tilde{V}_{ri}$ . This provides an independent estimate for the ion fluctuation-driven flux  $\Gamma_i^{\text{fl}} = \langle \tilde{n} \tilde{V}_{ri} \rangle$ , where the angular brackets represent time averaging over a sufficient number of fluctuation periods.

The fluctuation-induced flux for the electrons is assumed a result solely of  $\tilde{E} \times B$ , where the main contribution comes from the poloidal  $\tilde{E}$  component ( $\tilde{E}_p$ ) and the

toroidal  $B$  component ( $B_t$ ). Thus, the electron fluctuation-driven flux is given by  $\Gamma_e^{fl} = \langle \tilde{n} \tilde{E}_p \rangle / B_t$ .

To estimate the two species fluctuation-driven fluxes we require  $T_e$ ,  $T_i$ , and  $\tilde{E}_p$ . The ion temperature has been estimated using a retarding field energy analyzer [8]. Alternatively, an estimate of the local time-averaged density  $n_e$ , which is obtained using the multichannel spectroscopy diagnostic [13], allows an estimate of  $T_i$  directly from the ion saturation currents, since  $I_s \sim n_e \sqrt{T_e + T_i}$ . Either method allows the ion thermal velocity  $V_{ti}$  required for Eq. (2) to be determined. Both methods give reasonable agreement.

Triple probes provide a measurement of  $T_e$  and the plasma potential  $\phi_p$  [14]. The poloidal electric field is estimated from two poloidally separated triple probes as  $\tilde{E}_p = (\phi_{p2} - \phi_{p1}) / \Delta y$ , where  $\Delta y = 30$  mm is the distance between the probes.

To measure all the necessary quantities to independently estimate the two fluctuation-driven fluxes, we require a probe complex (see Fig. 1). This probe consists of a radial Mach probe surrounded in the poloidal direction by two triple probes. Simultaneously we measure the radial electric field using a ‘‘fork’’ probe. It consists of two triple probes constructed similarly as the probe in Fig. 1, but separated radially (rather than poloidally) by  $\Delta r \sim 15$  mm. The radial electric field is determined as  $E_r = (\phi_{r1} - \phi_{r2}) / \Delta r$ . Plasma fluctuations are dominated by coherent, low frequency ( $f \sim 5$ – $50$  kHz) pressure-gradient-driven resistive MHD modes and spectra may be found in Ref. [15]. Probe signals are digitized at 1 MHz, well above the observed fluctuation activity.

All five probes are radially and poloidally aligned using the electron beam mapping technique. Here we use the advantage of the stellarator vacuum magnetic structure.

Figure 2(a) shows the chord averaged density as measured by the 2 mm interferometer during an argon dis-

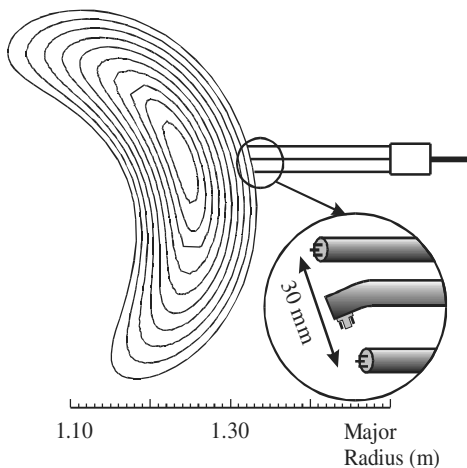


FIG. 1. Schematic of the triple-Mach probe complex. The tips of all three probes lie on the same flux surface. The central probe (Mach) is aligned to be sensitive to the radial flow. The inset shows an enlarged view of the probe tips.

charge with a spontaneous transition from low ( $L$ ) to high ( $H$ ) confinement modes [8]. In Fig. 2(b), the radial profile of the ion saturation current obtained in the  $L$  (triangles) and  $H$  (diamonds) modes is shown. One can see that the density rises considerably from  $L$  to  $H$  modes and that the gradient in the outer regions steepens. Figure 2(c) shows the root mean square (rms) of the fluctuations in the ion saturation current obtained in the  $L$  (triangles) and  $H$  (diamonds) modes. Fluctuation levels drop by more than a factor of 10 from the  $L$  to the  $H$  mode in the region of maximum fluctuation level.

In our experiments, we find that the major contribution to  $\tilde{V}_{ri}$  comes from  $\tilde{R}$ . Under most conditions,  $R$  has a time average  $\sim 1.1$  and fluctuates between approximately 0.9 and 1.3. Then  $\ln(R) = \bar{x} \pm \tilde{x} \sim 0.1 \pm 0.2$ . That is,  $\tilde{x}/\bar{x} \sim 2$  and, therefore,  $\tilde{R}$  tends to dominate even substantial fluctuations in either  $T_e$  or  $T_i$  ( $\tilde{T}/\bar{T} < 0.4$ ).

We find that the fluctuating ion radial velocity in the region of maximum density fluctuations is up to 10 times smaller than the measured  $\tilde{E} \times B$  drift. For example, at  $r/a \sim 0.4$ , the rms of the fluctuating ion radial velocity is less than 200 m/s, while the corresponding  $\tilde{E}_p/B_t$  is more than 2 km/s. Not surprisingly, the inferred estimates for the two fluctuation-driven fluxes also differ significantly in this region, as shown later in the Letter. In other words, the fluctuations produce a flux that is nonambipolar. This nonambipolarity of the fluctuation-driven fluxes leads directly to a radial current being produced.

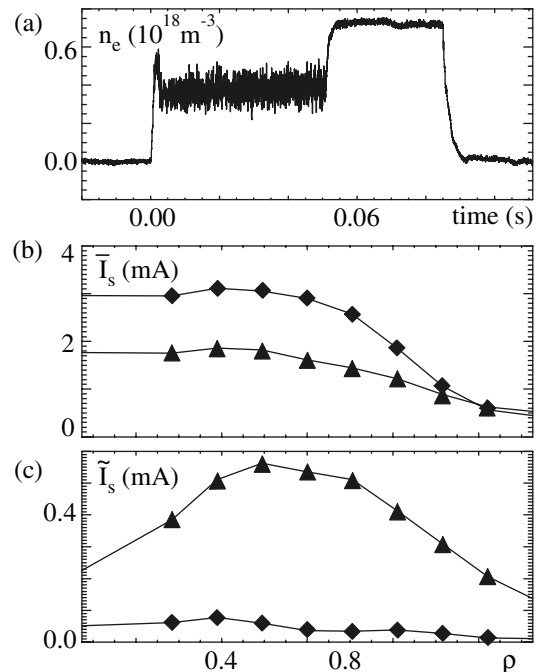


FIG. 2. (a) Chord average density from the 2 mm interferometer, measured in a shot with a spontaneous transition from low to high mode. (b) Radial profile of ion saturation current in the  $L$  (triangles) and the  $H$  (diamonds) modes. (c) Radial profile of the fluctuation level in ion saturation current in the  $L$  (triangles) and  $H$  (diamonds) modes.

Strictly speaking, the fluctuation-driven fluxes that we measure are local fluxes, which could arguably be different from the flux-surface-averaged fluxes. Nonetheless, measurements at other toroidal and poloidal locations reveal the same tendency. The fluctuating ion radial velocity (and subsequently the ion fluctuation-driven flux) remains substantially smaller than the electron counterpart does.

Existence of the radial current driven by fluctuations suggests that the physical mechanism leading to the confinement transitions from the *L* to the *H* mode in H-1 should be revised. In this case, the picture that fluctuations are suppressed, transport is reduced, and confinement improves is not quite applicable, since turning fluctuations off predominantly affects the electron flux.

Consider what must occur during a spontaneous transition from low to high confinement modes as in Fig. 2(a). Prior to the transition, the plasma is in steady state and Poisson's equation becomes

$$\frac{\varepsilon_0 \varepsilon_{\perp}}{e} \frac{\partial}{\partial t} E_r = \Gamma^{\text{AN}} + \Gamma^{\text{others}} = 0, \quad (3)$$

where  $\Gamma^{\text{AN}} = \Gamma_e^{\text{fl}} - \Gamma_i^{\text{fl}}$  is the nonambipolar anomalous flux and  $\Gamma^{\text{others}}$  is intended to represent all other fluxes, which may, for example, include  $\Gamma_e^{\text{NC}}$ , the electron neo-classical flux and  $\Gamma_i^{\text{OL}}$ , the ion orbit loss. So  $\Gamma^{\text{others}} = -\Gamma^{\text{AN}}$  balances the anomalous nonambipolar flux. A spontaneous transition from the low to the high mode occurs in approximately  $\Delta t \sim 1$  ms. During this time, the fluctuations are suppressed and subsequently  $\Gamma^{\text{AN}}$  drops out from Eq. (3). This leaves an imbalance in the Poisson equation, which we may approximate over this transition time as

$$\frac{\varepsilon_0 \varepsilon_{\perp}}{e} \frac{\Delta E_r}{\Delta t} = -\Gamma^{\text{AN}}. \quad (4)$$

This may be solved to estimate the change expected in the radial electric field in going from the low to the high mode across the transition.

Figure 3(a) shows the inferred electron fluctuation-driven flux (diamonds) during a radial scan in the *L* mode (just below the magnetic field threshold for the *H* mode). The corresponding ion flux in the *L* mode is shown in triangles. The nonambipolarity of the fluctuation-driven fluxes is quite evident. Note that  $\Gamma_e^{\text{fl}}$  is negative (inwards) in the inner two-thirds of the plasma and reverses to outwards in the outer third. In the inner region of the plasma, the measurements therefore show a fluctuation induced pinch of particles, particularly for the electrons. The squares show the electron fluctuation-driven flux in the *H* mode, which is reduced by nearly 2 orders of magnitude.

Figure 3(b) shows the radial profile of  $E_r$  as measured during an *L*-mode scan (diamonds). It is remarkably featureless over most of the plasma radius, until the outer few centimeters ( $r/a = 0.8-1.0$ ), where it becomes largely negative. This is seemingly to compensate ions whose gyro

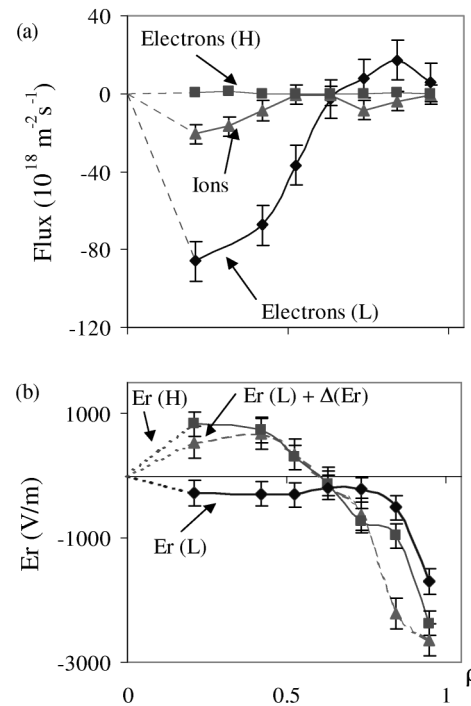


FIG. 3. (a) Radial profiles of the inferred fluctuation-driven flux in the *L* mode for electrons (diamonds) and ions (triangles) and in the *H* mode for electrons (squares). (b) Radial profiles of the radial electric field in the *L* mode (diamonds) and in the *H* mode (squares). The dashed profile (triangles) represents  $E_r(L) - (e\Gamma^{\text{AN}}\Delta t)/(\varepsilon_0\varepsilon_{\perp})$ .

orbits cross the last closed flux surface and are therefore readily lost in this region. The electric field in the quiescent high mode is also shown in Fig. 3(b), plotted with squares. In this mode, the electric field develops a substantial shear throughout the outer two-thirds of the plasma. The dashed profile in triangles in Fig. 3(b) shows the *L*-mode radial electric field  $E_r(L)$  plus the contribution  $\Delta E_r$  expected from the suppression of the nonambipolar anomalous flux, according to Eq. (4). This expected  $E_r(L) + \Delta E_r$  and the measured *H*-mode radial electric field  $E_r(H)$  are in good agreement. This is consistent with the fact that the fluctuation-induced fluxes are nonambipolar and lead to a radial current. In particular, the observed  $\Delta E_r$  (positive in the inner region, negative in the outer region) agrees with the direction of the anomalous fluxes. When the plasma is dynamically readjusting itself from the low to the high mode, the balance is lost and the radial electric field changes accordingly. During the change in  $E_r$ , other plasma transport processes also adjust as a result of  $E_r$ , and they eventually establish a new balance in the *H* mode.

In this picture, the causality of the spontaneous *L*-*H* transition [like the one shown in Fig. 2(a)] should be as follows. Close to the threshold conditions for the suppression of the fluctuation-driven transport,  $E_r$  (or its shear) dynamically increases [16]; the nonambipolar  $\Gamma^{\text{AN}}$  (or, in fact, the turbulent-driven radial current) is reduced, leading to a further increase in  $E_r$  shear. This  $E_r$  shear reduces

ion orbit loss, as shown in simulations [17], leading to the improved confinement and peaking in the density profile.

It has been noted [2] that the flux driven by electrostatic fluctuations in the plasma can be nonambipolar. Several mechanisms can lead to this nonambipolarity. For example, FLR effects [5,6] reduce the ion radial velocity. In particular, the electric field is averaged out over the ion gyro orbit and so the  $E \times B$  drift is reduced to

$$\tilde{V}_{ri} = \left(1 + \frac{1}{4} \rho_i^2 \nabla^2\right) \frac{\tilde{E}_p}{B}. \quad (5)$$

The FLR effect slows down ions such that  $\tilde{V}_{ri} < \tilde{V}_{re}$  and, therefore, the fluctuation-driven fluxes become nonambipolar. In the region of maximum density fluctuations,  $k_p \sim 20 \text{ m}^{-1}$ , and the ion Larmor radius is  $\rho_i \sim 6 \text{ cm}$ . The reduction due to FLR effects, from Eq. (5), should be less than 40%, although for higher  $k_p$  the effect will be stronger. It appears that FLR alone is not sufficient to account for the observed reduction of  $V_{ri}$ , and other damping mechanisms must be present.

The polarization drift,  $\tilde{V}_p = (M/eB^2)(dE_r/dt)$  is of similar magnitude to the  $E \times B$  velocity in our experiments and can also lead to the nonambipolarity in the turbulent particle flux [5]. Because of the difficulty in determining the phase of  $dE_r/dt$  from the experimental signals, it is not possible for us to quantify its contribution to the ion velocity reduction.

The nonambipolarity of the fluctuation-driven particle transport reported here can also be due to the damping of the large-scale ( $k_p \sim 10\text{--}20 \text{ m}^{-1}$ )  $E \times B$  flows of ions. It has been reported previously [8] that mean poloidal ion flows in H-1 are also heavily damped. Magnetic pumping processes have been shown to be responsible for the flow damping in toroidal devices [18]. This effect is expected to be particularly strong in H-1, which has a very high magnetic field ripple along the field line,  $\tilde{B} \sim (0.4\text{--}0.5)|B_0|$ . From this point of view, it is not surprising that the time-varying fluctuation-driven flows are also strongly damped.

A reduction in one of the fluctuating velocities is not the only way to generate a nonambipolar fluctuation-driven flux. Fluctuations can induce Reynolds stress, and this is known to generate flows [4]. Experimental measurements of the Reynolds stress in stellarators [19,20] have been shown to be comparable to the mean flow acceleration. One can attribute the radial current associated with the nonambipolarity of the fluxes as the driving mechanism of the flow. In our measurements, we can estimate the effective radial current due to the Reynolds stress as [4]

$$J_r = \frac{m_i n_e}{eB} \frac{\partial}{\partial r} \langle \tilde{V}_{ri} \tilde{V}_{pi} \rangle. \quad (6)$$

We estimate the contribution from the Reynolds stress using fluctuating ion velocities in both radial  $\tilde{V}_{ri}$  and po-

loidal  $\tilde{V}_{pi}$  directions measured with radially and poloidally oriented Mach probes (not simultaneously). The current calculated from (6) can be only about 10% of the nonambipolar fluctuation-driven current,  $J_r^{fl} = e(\tilde{\Gamma}_e^{fl} - \tilde{\Gamma}_i^{fl})$ , and is therefore not the dominant mechanism for generating the nonambipolar current in these experiments.

This Letter presents the first experimental confirmation of the possibility of nonambipolar fluctuation-driven flux. Individual estimates of the electron and ion fluctuation-driven fluxes are made in this Letter to make the comparison. The ion fluctuation-driven flux is determined using a radial Mach probe, while the electron fluctuation-driven flux is assumed to be due to the  $\tilde{E} \times B$  drift. The fluctuating radial ion velocity is considerably smaller than the corresponding electron quantity, and subsequently the fluxes are found to be nonambipolar. It is shown that the modification of the radial electric field from the low to the high mode is consistent with the suppression of the radial current in the region where the fluctuation transport is maximal. Therefore, fluctuations are shown to directly affect the structure of the radial electric field.

We thank J. H. Harris for useful discussions, A. Gough for assistance in the probe design, and the H-1 team for support during the experiments.

---

\*Electronic address: Wayne.Solomon@anu.edu.au

- [1] B. A. Carreras, IEEE Trans. Plasma Sci. **25**, 1281 (1997).
- [2] K. Itoh and S. I. Itoh, Plasma Phys. Controlled Fusion **38**, 1 (1996).
- [3] P. W. Terry, Rev. Mod. Phys. **72**, 109 (2000).
- [4] P. H. Diamond and Y. B. Kim, Phys. Fluids B **3**, 1626 (1991).
- [5] R. E. Waltz, Phys. Fluids **25**, 1269 (1982).
- [6] T. E. Stringer, Nucl. Fusion **32**, 1421 (1992).
- [7] S. M. Hamberger *et al.*, Fusion Technol. **17**, 123 (1990).
- [8] M. G. Shats *et al.*, Phys. Plasmas **4**, 3629 (1997).
- [9] B. J. Peterson *et al.*, Rev. Sci. Instrum. **65**, 2599 (1994).
- [10] E. Thomas *et al.*, Phys. Plasmas **5**, 3991 (1998).
- [11] M. Hudis and L. M. Lidsky, J. Appl. Phys. **41**, 5011 (1970).
- [12] W. M. Solomon and M. G. Shats, Rev. Sci. Instrum. **72**, 449 (2001).
- [13] H. Punzmann, M. G. Shats, and W. M. Solomon, Rev. Sci. Instrum. **72**, 965 (2001).
- [14] S. L. Chen and T. Sekiguchi, J. Appl. Phys. **36**, 2363 (1965).
- [15] M. G. Shats, Plasma Phys. Controlled Fusion **41**, 1357 (1999).
- [16] D. L. Rudakov *et al.*, Plasma Phys. Controlled Fusion **43**, 559–570 (2001).
- [17] J. L. V. Lewandowski, Phys. Plasmas **5**, 4101 (1998).
- [18] S. P. Hirshman and D. J. Sigmar, Nucl. Fusion **21**, 1079 (1981).
- [19] P. G. Matthews *et al.*, Phys. Fluids B **5**, 4061 (1993).
- [20] C. Hidalgo *et al.*, Phys. Rev. Lett. **83**, 2203 (1999).